Simulation and training of lumbar punctures using haptic volume rendering and a 6DOF haptic device

Matthias Färber, Julika Heller, and Heinz Handels

Department of Medical Informatics, University Medical Center Hamburg-Eppendorf
Martinistraße 52, 20246 Hamburg, Germany

ABSTRACT

The lumbar puncture is performed by inserting a needle into the spinal chord of the patient to inject medicaments or to extract liquor. The training of this procedure is usually done on the patient guided by experienced supervisors. A virtual reality lumbar puncture simulator has been developed in order to minimize the training costs and the patient's risk. We use a haptic device with six degrees of freedom (6DOF) to feedback forces that resist needle insertion and rotation. An improved haptic volume rendering approach is used to calculate the forces. This approach makes use of label data of relevant structures like skin, bone, muscles or fat and original CT data that contributes information about image structures that can not be segmented. A real-time 3D visualization with optional stereo view shows the punctured region. 2D visualizations of orthogonal slices enable a detailed impression of the anatomical context. The input data consisting of CT and label data and surface models of relevant structures is defined in an XML file together with haptic rendering and visualization parameters. In a first evaluation the visible human male data has been used to generate a virtual training body. Several users with different medical experience tested the lumbar puncture trainer. The simulator gives a good haptic and visual impression of the needle insertion and the haptic volume rendering technique enables the feeling of unsegmented structures. Especially, the restriction of transversal needle movement together with rotation constraints enabled by the 6DOF device facilitate a realistic puncture simulation.

Keywords: Procedure simulation, Surgical Simulation, Visualization, Virtual Reality, Haptic feedback, Lumbar puncture

1. INTRODUCTION

This section gives a short overview about the lumbar puncture and how it is trained. Furthermore a survey of related work is given.
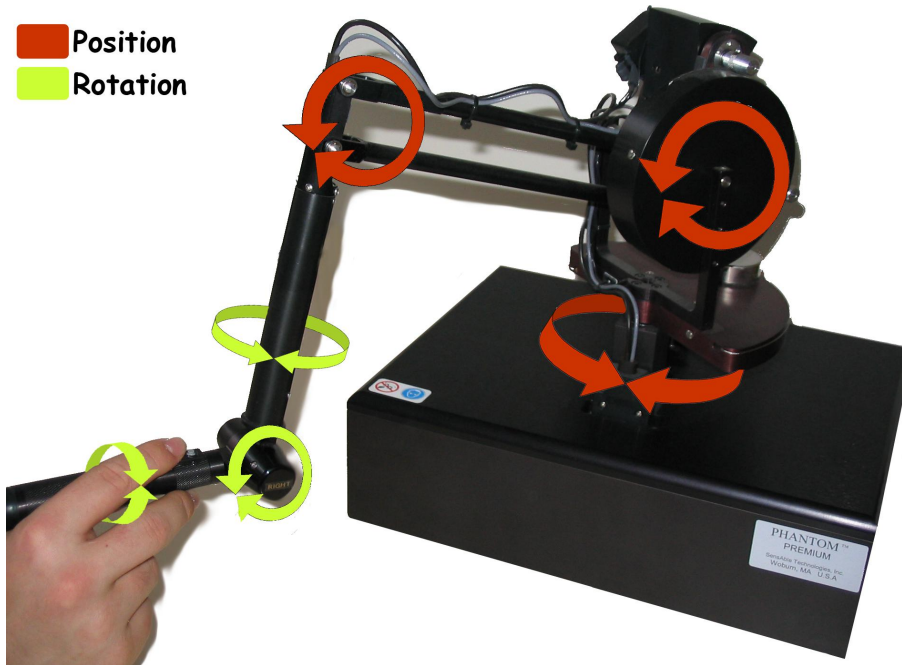
1.1. Lumbar puncture

Lumbar punctures are performed for diagnostic purposes and therapy. The puncture is done by inserting a needle into the spinal chord to inject medicaments or to extract liquor. A thin biopsy needle is inserted, usually between the lumbar vertebrae L3/L4 or L4/L5 and pushed in until there is a haptic feedback, a sort of "give", that indicates the needle is inside the spinal chord. Serious complications of a lumbar puncture like spinal or epidural bleeding, and trauma to the spinal cord or spinal nerve roots are rare. The lumbar puncture can cause pain when the needle hits bone structures. Like in most other medical procedures, experience in doing lumbar punctures helps to avoid inconveniences and risks for the patient. Therefore a good training of this procedure is essential for a successful lumbar puncture.

1.2. Training of lumbar punctures

Lumbar punctures are usually trained guided by experienced supervisors directly on the patient. Clinicians then improve their skills "learning by doing". The use of training dolls or cadavers is unusual. In most cases beginners only have theoretical knowledge from books. Recently the relevance of virtual reality (VR) based simulators is increasing because with the use of simulators experience can be gained cheaply without risking the patient's health.

---

*Correspondence: E-mail: mfaerber@uke.uni-hamburg.de; WWW: http://www.uke.de/imi; Telephone: +49 (0)40 42803 7792; Fax +49 (0)40 42803 4882

Figure 1. Sensable's Phantom Premium device with 6 degrees of freedom

1.3. Related work

Recent lumbar puncture simulators[1–5] use precomputed virtual haptic models generated from segmented image data. Haptic feedback of structures that have not been segmented or modelled can not be rendered. Our approach combines original CT data with label data to facilitate the haptic feedback of structures that can not be segmented with common methods. Furthermore the use of a haptic device with six degrees of freedom for puncture simulation is new and e.g. enables the haptic rendering of torques and forces that resist needle rotation and transversal needle movement.

2. PUNCTURE SIMULATION FRAMEWORK

Our training system presents a virtual scene that consists of a user-steered virtual needle and a virtual body generated from segmented CT data. The simulation is split up into a haptic and a visual component.

2.1. Haptic component

The haptic component renders the forces that affect the needle during the insertion. The forces are calculated in real-time depending on needle position, needle rotation, insertion angle and local tissue properties. The haptic device is then used to return the rendered forces to the user.

2.1.1. Haptic Device

A force feedback device with six degrees of freedom (Sensable Phantom Premium 1.5) is used for the haptic I/O. This device enables haptic feedback in three directions in space and in three rotation axes of the pen-like end effector (fig. 1). The nominal position resolution of this device is 860 dpi for translation sensing, 0.0023 degrees for yaw and pitch rotation and 0.008 degrees for roll rotation. The translational force output is limited to 8.5 N maximum (peak force) and 1.4 N continuous force output. The maximum exertable torque is 515 mNm for yaw and pitch and 170 mNm for roll. The continuous exertable torques are 188 mNm and 48 mNm respectively.

2.1.2. Proxy-based haptic volume rendering

The forces that affect the needle during the insertion are calculated based on a proxy based haptic volume rendering approach.[6,7] The use of virtual proxys[8] or god-objects[9] is a common method for haptic surface rendering, because it allows smooth shaded feedback from unprocessed polygons. The basic idea behind proxy-based methods is that a virtual spring damper with damping constant k connects the haptic instrument to a virtual proxy. By the restriction of proxy movement forces are indirectly (by the spring) applied to the haptic instrument using Hooke's law

$$\vec{f} = -k\vec{d} \tag{1}$$

where $\vec{d}$ is the distance between proxy position $\vec{x}_p$ and instrument position $\vec{x}_t$. While in haptic surface rendering planes defined by the surface normals restrict the proxy from moving through surfaces, in proxy based haptic volume rendering the proxy is constrained to move only perpendicular to the gradient vector at the proxy position $\vec{\nabla}V(\vec{x}_p)$ (fig. 2).
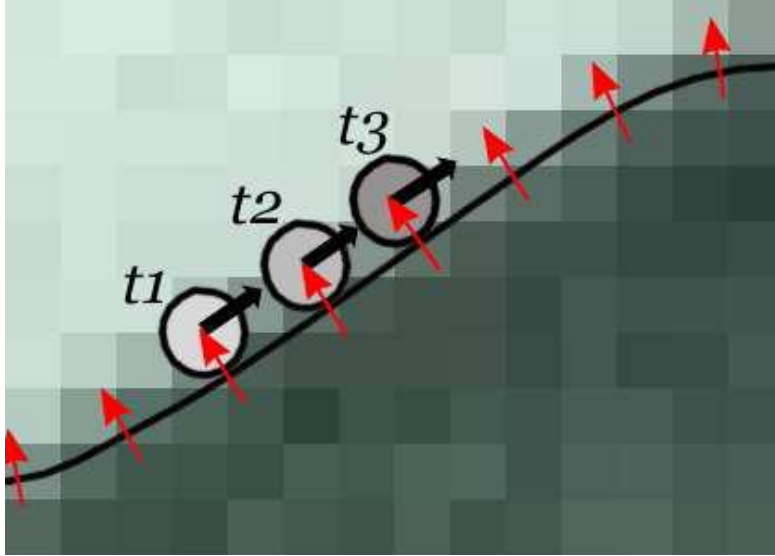
Figure 2. Proxy-based haptic volume rendering: The proxy is constrained to move only perpendicular to the gradient vector

In detail, the force vector $\vec{f}$ from the spring simulation is split up in two orthogonal portions $\vec{f}_N = \vec{f} \cdot \hat{N}$ and $\vec{f}_T = \vec{f} \cdot \hat{T}$ where

$$\hat{N} = \frac{\vec{\nabla}V(\vec{x}_p)}{\left|\vec{\nabla}V(\vec{x}_p)\right|} \quad \text{and} \quad \hat{T} = \frac{\vec{d} - \hat{N}\left(\vec{d} \cdot \hat{N}\right)}{\left|\vec{d} - \hat{N}\left(\vec{d} \cdot \hat{N}\right)\right|} \quad . \tag{2}$$

The new proxy position $\vec{x}_p'$ is calculated in every time step (approx. 1000 times per sec.). The movement is split up into three steps that correspond to the simulation of penetrability (eq. 3), friction (eq. 4) and viscosity (eq. 5).

$$\vec{x}_p' = \begin{cases} \vec{x}_p + \hat{N}(\vec{d} \cdot \hat{N} - T_N/k) & \text{if } T_N < k(\vec{d} \cdot \hat{N}) \\ \vec{x}_p & \text{otherwise} \end{cases} \tag{3}$$

$$\vec{x}_p' = \begin{cases} \vec{x}_p + \hat{T}(\vec{d} \cdot \hat{T} - T_T/k) & \text{if } T_T < k(\vec{d} \cdot \hat{T}) \\ \vec{x}_p & \text{otherwise} \end{cases} \tag{4}$$

$$\vec{x}_p' = \begin{cases} \vec{x}_p + \frac{R(\vec{X}_{pO} - \vec{x}_p)}{k|\vec{X}_{pO} - \vec{x}_p|} & \text{if } R/k < |\vec{X}_{pO} - \vec{x}_p| \\ \vec{x}_{pO} & \text{otherwise} \end{cases} \tag{5}$$

$\vec{x}_{pO}$ is the original position of the proxy at the beginning of the time step. T_T and T_N are thresholds that define how the proxy sticks to its current position and R and k are the constants for viscosity and spring elasticity. These thresholds and constants can be used to define material properties like friction, stiffness, viscosity and penetrability by using them as transfer functions (e.g. $k = K_{tf}(V(\vec{x}_p))$). Figure 3 illustrates the stepwise proxy movement as described in.[6] First the proxy is moved (or not moved) in direction of the surface normal to simulate penetrability. Then the proxy is moved perpendicular to the surface normal to generate the friction effect. Finally a repositioning back to the initial proxy position $\vec{x}_{pO}$ is done to simulate viscosity.
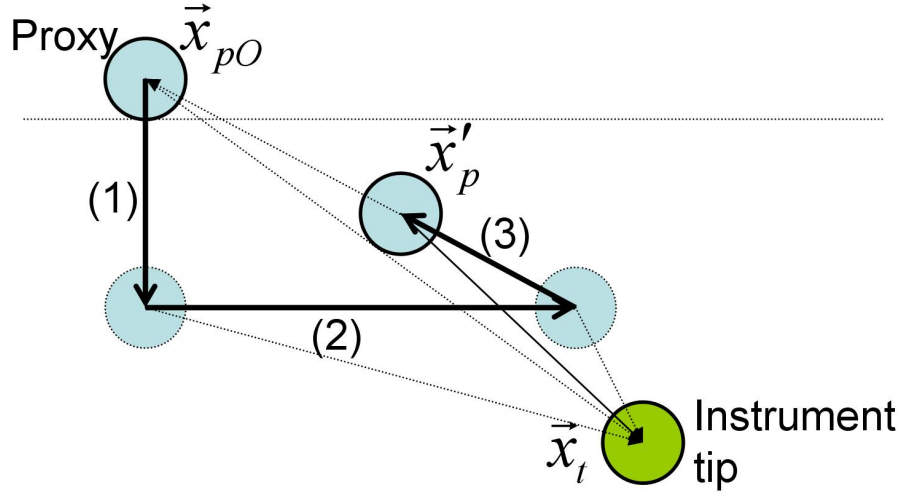

Figure 3. The proxy movement to simulate: 1) penetrability, 2) friction and 3) viscosity

2.1.3. Needle tip forces

The surface resisting force (fig. 4(a)), surface friction (fig. 4(b)), and viscosity (fig. 4(c)), that affect the needle tip, are calculated using the haptic volume rendering approach. We extended the method described in 2.1.2 so that it combines information from label data $V_L(\vec{x})$ with information given by original CT data $V_{CT}(\vec{x})$. It is possible to ensure haptic feedback from structures that are essential for a realistic haptic sensation by segmenting these structures manually. This sensation is extended by the haptic feedback from structures that are represented in CT density data. We combine the label data $V_L(\vec{x})$ and CT data $V_{CT}(\vec{x})$ to build up a new image $V(\vec{x})$ additively. We define the values that are used to mark structures like bone, skin, muscles, or fat in the label data $V_L(\vec{x})$ in such a way that a realistic haptic feedback is generated by the haptic volume rendering approach.

2.1.4. Needle body forces

The realistic behaviour of the needle is improved by restricting rotation (fig. 4(d)) and transversal motion (fig. 4(e)) of the needle inside the body. Furthermore a friction force (fig. 4(f)), that resists the needles body from sliding through the tissue is computed based on the penetration depth. The needle position and needle direction vectors $\vec{p}$ and $\vec{d}$ are stored at the moment the needle pierces the skin to calculate correction forces that restrict the user from rotating the needle inside the body and transversal needle movement. Transversal motion of the needle is restricted using a spring force technique. The position of the proxy $\vec{x}_p$ after the calculation of the needle tip forces (2.1.3 and 2.1.2) is projected onto the straight line defined by $\vec{p}$ and $\vec{d}$ (fig. 5). The torque values that control the rotational axes of the 6DOF haptic device are calculated using a quaternion that transforms the current needle direction vector $\vec{d}_c$ to $\vec{d}$. The current penetration depth is used to compute an amplifying factor for the torque forces so that the restriction of needle rotation depends on the depth of needle insertion.
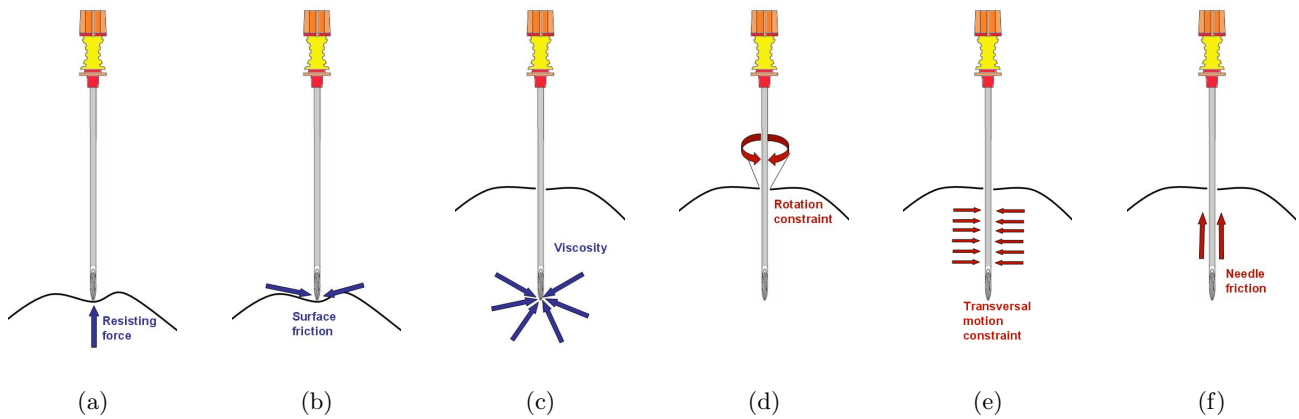
**Figure 4.** Needle tip forces (a)-c)) and needle body forces (d)-f))

2.2. Visual component

2D and 3D visualizations of the virtual body build up the visual component

The 3D scene shows a virtual representation of the needle and the surfaces of relevant medical structures (fig. 6). The organ surfaces can be generated using the label data $V_L(\vec{x})$ announced in 2.1.3. Visualization techniques using different colours and opacities for each organ can be used to give a concise impression of the anatomical coherences. The whole scene can be rotated, panned and zoomed using the mouse. An optional stereo view improves the impression of depth in the virtual body.

Three 2D views show orthogonal slices (sagittal, coronal and axial) of the image data (fig. 7). The slice positions are defined by the current position of the needle tip. The alignment of the needle is shown by a projection of the needle direction vector $\vec{d}$ into each orthogonal view.

An XML file is used to provide the application with the label data $V_L(\vec{x})$, the CT-image data $V_{CT}(\vec{x})$, surface data of all relevant structures, and a three-dimensional representation of the needle. Furthermore the visualization parameters like surface colours and opacities for each surface and the initial viewing position are
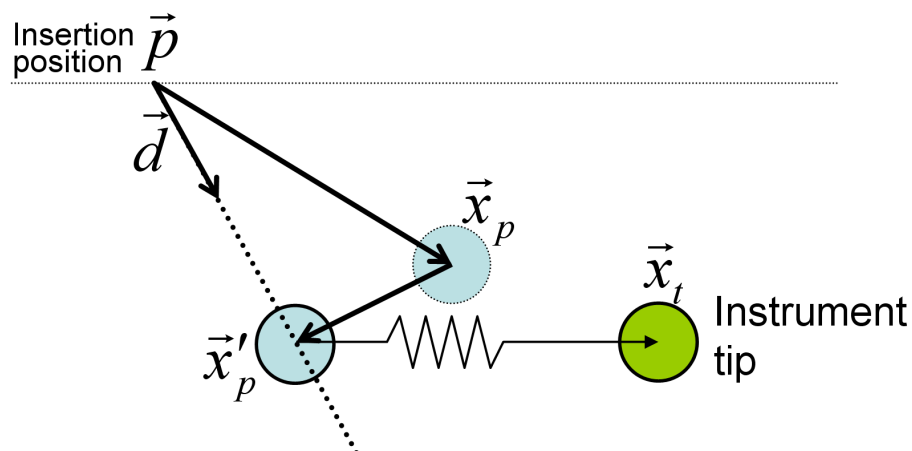
Figure 5. Restriction of transversal movement by projecting the proxy position $\vec{x}_p$ on to the insertion line defined by $\vec{p}$ and $\vec{d}$.
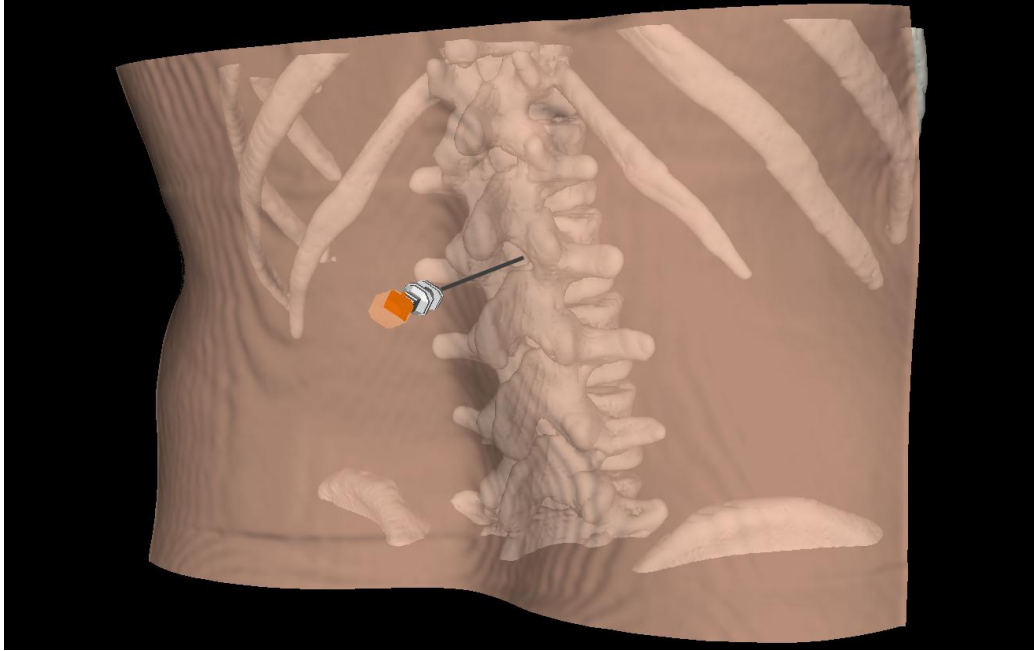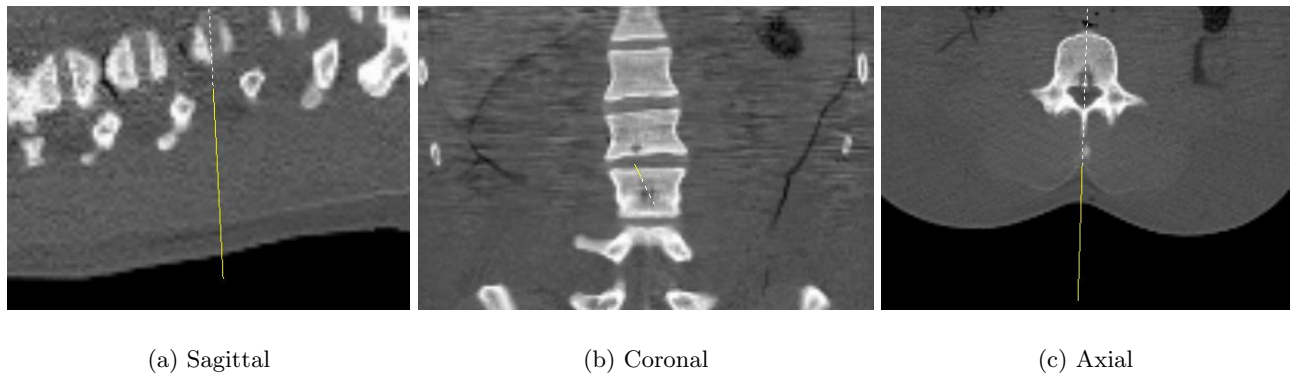
Figure 6. 3D visualization showing the virtual patient and the virtual needle

defined. The friction, viscosity and penetrability parameters are defined for each structure to enable a realistic haptic impression.

3. RESULTS

The input data for the lumbar puncture simulator has been generated based on the visible human male data set.[10] We used the CT data and the segmentations (label data) of skin, bone, muscles, ligaments, fat and target area. Surface models have been generated based on the label data to enable the 3D visualization. Parameters for haptic and visual component and the definition of the input data are provided to the framework using the XML file.

Several users with varying medical experience tested the simulation of lumbar puncture. The users were able to identify different tissues like muscles, fat, skin and bone by means of viscosity, resisting force and friction. The
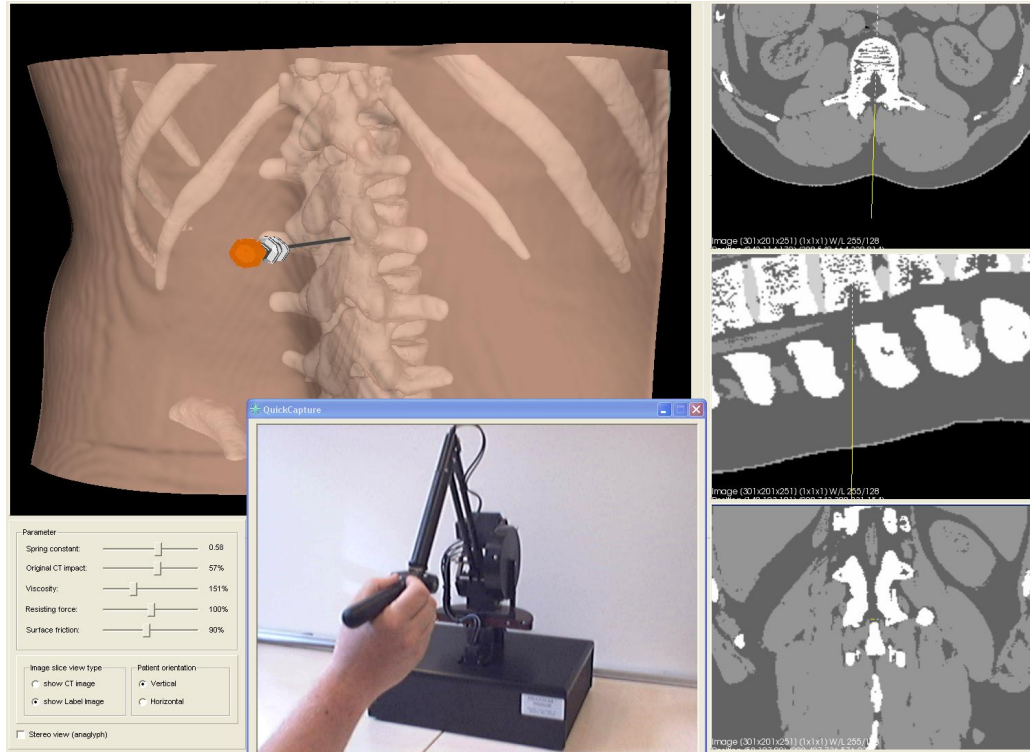

(a) Sagittal   (b) Coronal   (c) Axial

Figure 7. 2D visualization showing orthogonal slices and a projection of the virtual needle

Figure 8. User interface of the lumbar puncture system showing a 3D visualization of needle, opaque skin and bone as well as orthogonal slices (axial, sagittal, and coronal) each crossing the virtual volume at the current position of the needle tip. The current position of the haptic device is shown by a webcam snapshot.

extended haptic volume rendering technique facilitated force feedback from labelled and unsegmented structures. The restriction of transversal needle movement together with the rotation constraints enabled by the 6DOF device facilitated a realistic needle behaviour. The synchronization of force feedback and miscellaneous visualization techniques provided a realistic impression of the anatomy though most users were unfamiliar with the usage of a haptic device. The use of virtual reality techniques opens up new opportunities to support and improve the lumbar puncture training in medical education.

4. CONCLUSIONS AND FUTURE WORK

The virtual reality simulator presented supports a realistic training of lumbar punctures in virtual bodies. The training method offers a new way of understanding human anatomy and gaining experiences in using a puncture needle. Our visualization techniques enable the user to look inside the body. This helps to understand the human anatomy of the punctured region and to verify the needle placement. The haptic component provides a realistic needle handling. Nevertheless some aspects of a real lumbar puncture like communication with the patient or palpation can not be simulated. Therefore the use of a virtual training system can not replace the direct training on the patient. It should rather be considered as enhancement of the usual training methods that supports the users in preparing their first real lumbar punctures.

Soft tissue deformations have been neglected in our approach since only small deformations arise during the lumbar puncture. Nevertheless the definition of haptic properties like stiffness or friction for each segmented structure enables the user to identify tissues like skin or muscles as soft and structures like bones or ligaments as more solid.

The simulator is prepared to work with arbitrary patient data. We will exploit this feature by providing other lumbar puncture cases with different pathologies. This can help to train users in puncturing patients with abnormal or pathologic anatomy.

REFERENCES

1. P. Gorman, T. Krummel, R. Webster, M. Smith, and D. Hutchens, "A prototype haptic lumbar puncture simulator.," *Stud Health Technol Inform* **70**, pp. 106–109, 2000.
2. J. B. Ra, S. M. Kwon, J. K. Kim, J. Yi, K. H. Kim, H. W. Park, K.-U. Kyung, D.-S. Kwon, H. S. Kang, S. T. Kwon, L. Jiang, J. Zeng, K. Cleary, and S. K. Mun, "Spine needle biopsy simulator using visual and force feedback.," *Comput Aided Surg* **7**(6), pp. 353–363, 2002.
3. U. Dreifaldt, Z. Kulcsar, and P. Gallagher, "Exploring haptics as a tool to improve training of medical doctors in the procedure of spinal anaesthetics," in *Eurohaptics*, (Paris), July 2006.
4. T. Dang, T. M. Annaswamy, and M. A. Srinivasan, "Development and evaluation of an epidural injection simulator with force feedback for medical training.," *Stud Health Technol Inform* **81**, pp. 97–102, 2001.
5. L. Hiemenz, D. Stredney, and P. Schmalbrock, "Development of the force-feedback model for an epidural needle insertion simulator.," *Stud Health Technol Inform* **50**, pp. 272–277, 1998.
6. K. Lundin, A. Ynnerman, and B. Gudmundsson, "Proxy-based haptic feedback from volumetric density data," in *Eurohaptics Conference*, pp. 104–109, (University of Edinburgh, United Kingdom), 2002.
7. K. Lundin, B. Gudmundsson, and A. Ynnerman, "General proxy-based haptics for volume visualization," in *World Haptics Conference*, pp. 557–560, (Pisa, Italy), 2005.
8. D. C. Ruspini, K. Kolarov, and O. Khatib, "The haptic display of complex graphical environments," in *Computer Graphics (SIGGRAPH 97 Conference Proceedings)*, pp. 345–352, ACM SIGGRAPH, 1997.
9. C. B. Zilles and J. K. Salisbury, "A constraint-based god-object method for haptic display," in *IROS '95: Proceedings of the International Conference on Intelligent Robots and Systems-Volume 3*, p. 3146, IEEE Computer Society, (Washington, DC, USA), 1995.
10. V. M. Spitzer and D. G. Whitlock, "The Visible Human Dataset: the anatomical platform for human simulation.," *Anat Rec* **253**, pp. 49–57, Apr 1998.
11. R. S. Avila and L. M. Sobierajski, "A haptic interaction method for volume visualization," in *Proceedings of the 7th conference on Visualization '96*, pp. 197–204, 1996.
12. O. Gerovich, P. Marayong, and A. M. Okamura, "The effect of visual and haptic feedback on computer-assisted needle insertion.," *Comput Aided Surg* **9**(6), pp. 243–249, 2004.